SWE, A COMPREHENSIVE PLASMA INSTRUMENT FOR THE WIND SPACECRAFT

K. W. OGILVIE, D. J. CHORNAY, R. J. FRITZENREITER, F. HUNSAKER,
J. KELLER, J. LOBELL, G. MILLER, J. D. SCUDDER and E. C. SITTLER, JR.
Interplanetary Physics Branch, Goddard Space Flight Center, Greenbelt, MA 20771, U.S.A.

R. B. TORBERT, D. BODET and G. NEEDELL
*Physics Department and Space Science Center, Institute for Study of Earth, Oceans, and Space,
University of New Hampshire, Durham, NH 03284, U.S.A.*

A. J. LAZARUS, J. T. STEINBERG and J. H. TAPPAN
Center for Space Research, Massachusetts Institute of Technology, Cambridge, MA 02139, U.S.A.

and

A. MAVRETIC and E. GERGIN
Microelectronics Research Laboratory, Boston University, Boston, MA 02215, U.S.A.

Abstract. The Solar Wind Experiment (SWE) on the WIND spacecraft is a comprehensive, integrated set of sensors which is designed to investigate outstanding problems in solar wind physics. It consists of two Faraday cup (FC) sensors; a vector electron and ion spectrometer (VEIS); a strahl sensor, which is especially configured to study the electron 'strahl' close to the magnetic field direction; and an on-board calibration system. The energy/charge range of the Faraday cups is 150 V to 8 kV, and that of the VEIS is 7 V to 24.8 kV. The time resolution depends on the operational mode used, but can be of the order of a few seconds for 3-D measurements. 'Key parameters' which broadly characterize the solar wind positive ion velocity distribution function will be made available rapidly from the GGS Central Data Handling Facility.

1. Introduction

The solar wind experiment (SWE) for the WIND spacecraft is a comprehensive, integrated set of instruments which will attack many outstanding problems in the magnetosheath, the foreshock, and the interplanetary medium. It also has the capability of making measurements in other regions which might become available to it.

The 'key parameters' (velocity, density, and temperature of the solar wind ions) will be extracted from detailed three-dimensional measurements made by the Faraday cup (FC subsystem; they will be made available rapidly through the GGS Central Data Handling Facility. This part of the instrument derives from the Voyager plasma instrument (Bridge *et al.*, 1977) and the Faraday cup instruments on IMP 7 and 8 (Bellomo and Mavretic, 1978). The FC subsystem is particularly suited for measurement of flowing, supersonic plasma such as that found in the interplanetary medium. Table I lists the key parameters and the expected measurement precisions.

TABLE I

Key parameters from the SWE instrument

Parameter	Range	Precision
Proton velocity (3 components)	200–1250 km s^{-1}	±3%
Proton number density	0.1–200/cc	±10%
Thermal speed	0–200 km s^{-1}	±10%
Alpha/proton number density ratio × 100	0–100%	±10%

The foreshock electrons and ions reflected from the bow shock will be studied using a vector electron and ion spectrometer (VEIS) derived from ISEE-1 instrumentation (Ogilvie *et al.*, 1978) but with increased sensitivity which is sufficient to make more detailed measurements. It will obtain highly-time-resolved, three-dimensional snapshots of the distribution functions of ions and electrons having energies/charge from 7 V to 24.8 kV for flowing plasmas with Mach numbers of unity and below.

A property of the solar wind electron velocity distribution which has not received sufficient study at 1 AU is the field-aligned distortion of the electron distribution function. That distortion, known as the 'strahl', has been interpreted to be a remnant of the electron distribution in the solar corona (Scudder and Olbert, 1979a, b) and is thus of considerable theoretical interest. The SWE has a specialized subsystem, the strahl detector, to study this phenomenon, by making detailed measurements of the electron velocity distribution near the direction of the magnetic field.

Such a comprehensive instrument, with many possible modes of operation, must be controlled by a correspondingly flexible data processing and control unit (DPU). The DPU, has ample computational capacity for the control of many possible modes, for data storage and formatting for presentation to the telemetry system, for command decoding, and for some data analysis. (For example, it is possible to calculate approximate key parameters on-board the spacecraft.)

This paper consists of a compact discussion of the scientific aims of the SWE, followed by a brief description of each of the subsystems; our intent is to give sufficient detail to allow preliminary assessment of the data obtained by them.

2. Scientific Objectives

The scientific aims of the investigation include those directly related to the GGS program of investigating the transfer of energy and momentum from the Sun to the earth and those which concern the properties of interplanetary space and are

independent of the presence of Eanh. We outline briefly the major objectives of our experiment in the following paragraphs.

2.1. STUDIES OF THE ENERGY AND MOMENTUM INPUT TO THE MAGNETOSPHERE

Of particular interest to the GGS program are measurements of the solar wind velocity (three components), density, and average thermal speed for which Faraday cups are especially suitable. The incoming energy and momentum available for transfer to the magnetosphere can then be computed (assuming that the single-point measurement at WIND is representative of conditions over the cross section of the magnetosphere), and changes in these quantities can be compared with time-correlated changes in the magnetosphere.

2.2. MAGNETOSPHERIC EFFECTS OF UPSTREAM WAVES AND PRESSURE CHANGES

There is currently abundant evidence that many magnetospheric phenomena are caused by a combination of changes in the bulk velocity and number density of the solar wind together with changes in the direction of the incident magnetic field. Those variations in the incident wind are often difficult to identify clearly as causes of specific magnetospheric events without observations upstream in the solar wind. The continuous coverage, good time resolution, and good determination of the bulk velocity, provided by the SWE are expected to provide inputs needed by magnetospheric modelers. The provision of these parameters are the main GGS-related scientific aim.

2.3. MEASUREMENTS IN THE REGION BETWEEN THE $L1$ LAGRANGIAN POINT AND THE BOW SHOCK

Even though WIND spends a good portion of its time far from Earth-related disturbances (such as ions reflected from the bow shock), it will still not be possible to correlate changes in the solar wind seen near $L1$ with magnetospheric events unless the region between $L1$ and the bow shock is thoroughly explored. That exploration should include identification of wave types and conditions for their generation so that the changes occurring as the solar wind approaches Earth can be incorporated in models which can then give a clear picture of the environment just upstream of the magnetosphere. Identification of the incoming waves requires the close, cooperative analysis of data from different WIND experiments as well as those from other spacecraft envisioned in the structure of GGS and made possible by ready access to data in the ground data system. The region upstream of the bow shock, called the 'foreshock', is described in a compilation 'Upstream Waves and Particles' in *J. Geophys. Res.* **86**, 4319, 1981.

2.4. BOW SHOCK AND MAGNETOSHEATH STUDIES

Studies of the bow shock and the magnetosheath, especially near the stagnation point, can be performed during the early part of the mission when the spacecraft makes multiple traversals of the bow shock region on both sides of the noon meridian. The (VEIS) and the Faraday cups (FC) together can cover a Mach number range from zero to at least 20; and the SWE has a mode in which traversals can be captured rapidly and played back more slowly. Of particular interest are studies of multiple crossings of the bow shock and evidence for reconnection events.

2.5. MEASUREMENT OF VELOCITY DISTRIBUTION FUNCTIONS OF PROTONS,
      HELIUM IONS, AND ELECTRONS

The SWE complement of sensors makes possible measurement of the three-dimensional velocity distribution functions of the protons and alphas. Two FC sensors provide cuts through the wind' s velocity distribution function integrated in a plane perpendicular to the cup normal (see, for example, Vasyliunas, 1971). The two Faraday cup normals are placed 15° above and below the equatorial plane of the spacecraft thus providing three-dimensional scans of the ion distribution function.

The VEIS instrument measures three-dimensional velocity distribution functions for flows with Mach numbers less than unity. The electrons in the solar wind, magnetosheath and magnetosphere, and ions reflected diffusely from the bow shock satisfy this condition. The instrument, derived from the electron spectrometer on the ISEE-1 spacecraft, can supply accurate meas- urements of the electron heat flux, including its direction and the flow direction of the electrons (see Figure 1). The SWE strahl sensor is able to make detailed measurements of the electron velocity distribution along the magnetic field direction where the distribution is distorted, reflecting the non-local nature of those electrons (see further discussion in Section 3.5).

2.6. HIGHLY-TIME-RESOLVED MEASUREMENTS OF THE SOLAR WIND

As discussed later, measurement of the entire ion velocity distributions can be made as the spacecraft rotation carries a Faraday cup with its wide acceptance angle of ±60° through the solar wind direction in approximately 1 s. This mode of operation promises to extend measurement of the solar wind parameters into a time regime that has not yet been thoroughly explored.

2.7. STUDIES OF INTERPLANETARY SHOCKS AND INTERACTION REGIONS

In addition to studying the nature of the bow shock, the 'burst' or 'event' mode of the SWE instrument can be used to observe phenomena in the vicinity of other boundaries in the plasma. In this mode, all subsystems are operated at their highest
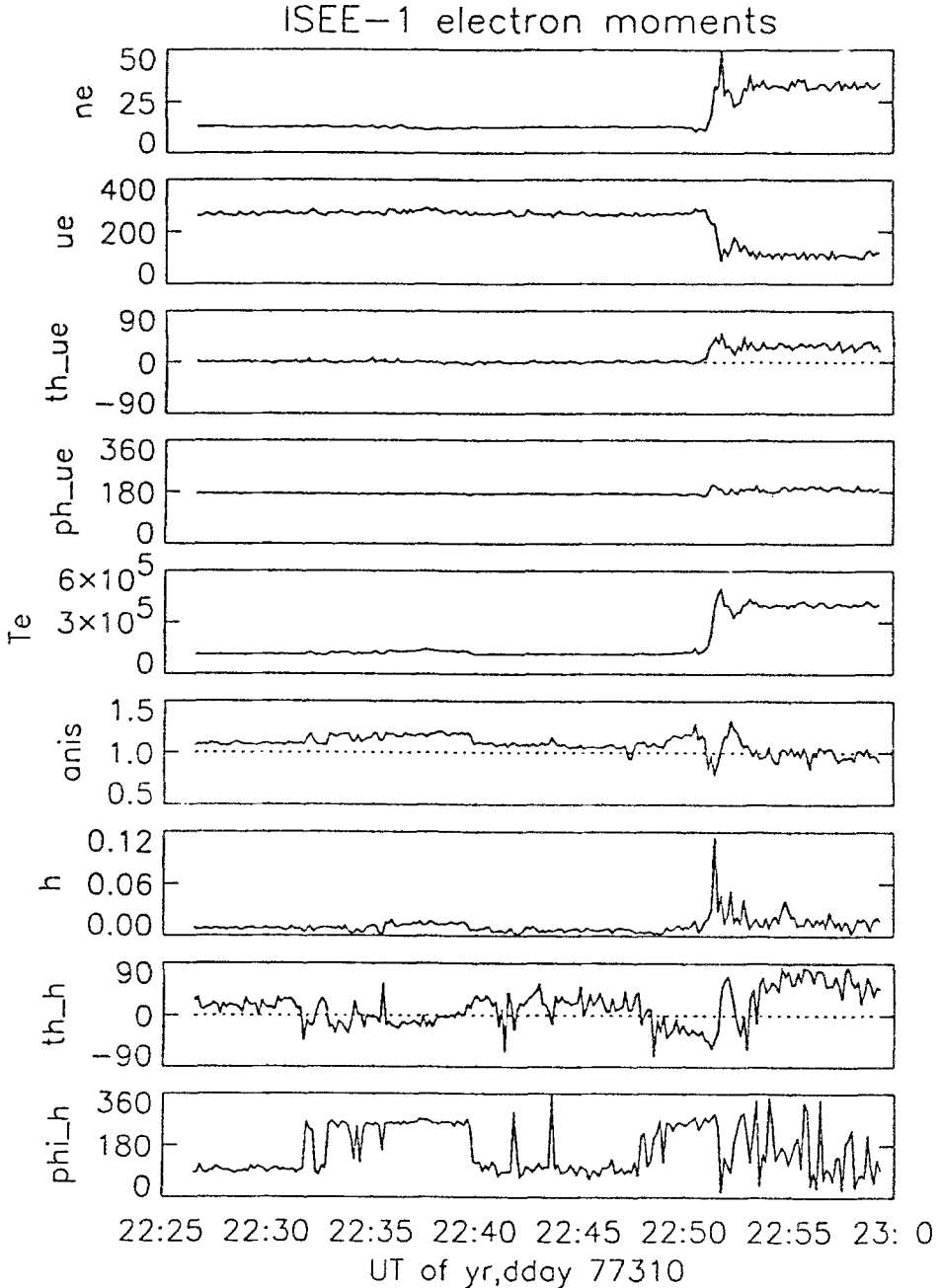
ISEE-1 electron moments

Fig. 1.   Quantities derived from electron observations made by the Vector Electron Spectrometer flown on the ISEE-1 spacecraft, which was similar to the VEIS to be deployed on the WIND spacecraft. Beginning in the top panel are shown electron density (ne); bulk speed (ue); elevation $(th - ue)$ and azimuth $(ph - ue)$ angles; electron temperature (Te); temperature anisotropy (anis), i.e., the parallel to perpendicular temperature ratio; heat flux (h); and its elevation (th h) and azimuth $(ph - h)$ angles. The data are from an inbound pass from the solar wind into the magnetosheath with a bow shock crossing at 22:52 UT. Note that in the solar wind (prior to 22:52 UT) the plasma density, flow speed, and direction are steady, but the heat flux shows several reversals in direction indicating multiple crossings of the electron foreshock. The electron temperature and anisotropy also show increases when crossing the foreshock.

time resolution keeping the data storage full. A short time after a 'trigger' condition is satisfied, data taking ceases so that observations both 'before' and 'after' are in the memory. The instrument then telemeters data at a reduced rate until the memory has been read out. Of considerable interest is the characterization of the microscale structure of shocks and of the interfaces between fast and slow solar wind that evolve into co-rotating interaction regions. Direct connections between the SWE, MFI, and WAVES experiments will allow complementary data triggers.

The 'event' mode will also be used to study the structure of the magnetopause and bow shock, using time-tagged commands, and to make rapid measurements of particle properties (such as correlations) for extended periods.

2.7.1. *Global studies of the heliospheric solar wind*

Interpretation of observations from spacecraft in the distant heliosphere (Voyager and Pioneer) and those beyond 1 AU and out of the ecliptic (Ulysses, Galileo, and future missions) requires a comparison with measurements near 1 AU where phenomena are better understood and long-term data bases are available. For example, the dynamic pressure variation of the wind can move the termination shock by as much as 10 AU in a single year (Belcher *et al.*, 1993). Such basic measurements near 1 AU will be provided in part by SWE and are an important part of the scientific aims of the experiment.

3. Instrument Description

3.1. GENERAL CONFIGURATION

The instrument consists of five sensors mounted in separate boxes, a Data Processing Unit (DPU), and a calibrator. Figure 2 shows how these components are mounted on the spacecraft. A Faraday cup and a triad of electrostatic analyzers (half the VEIS) are located at each end of a spacecraft diameter. One group of sensors is augmented by the strahl sensor. The DPU and calibrator are mounted between the two groups of sensors, near the middle of the spacecraft. Each group of sensors communicates with the DPU through an interface board contained in the VEIS housing. We describe each subsystem in more detail in the following sections. Table II lists some physical dimensions of the subsystem sensors and their relevant characteristics.

3.2. THE DPU

The DPU provides the only electrical interface with the spacecraft. It receives and interprets commands and controls the SWE subsystems using various pre-defined modes of operation. Flight software has been written for several measurement modes; the 'burst' mode has already been mentioned. A description of some of the modes is given in Section 4.
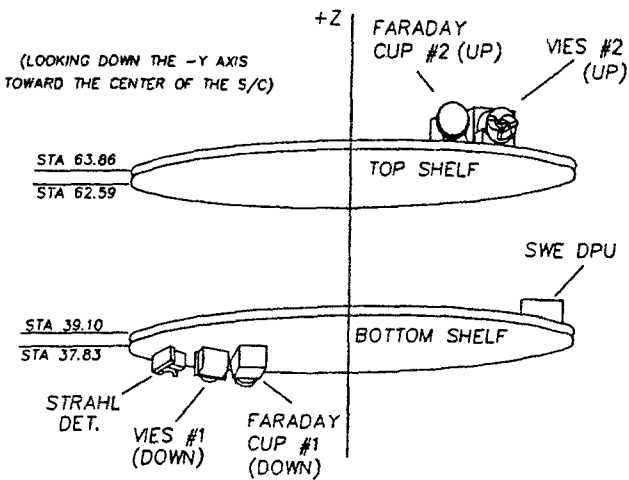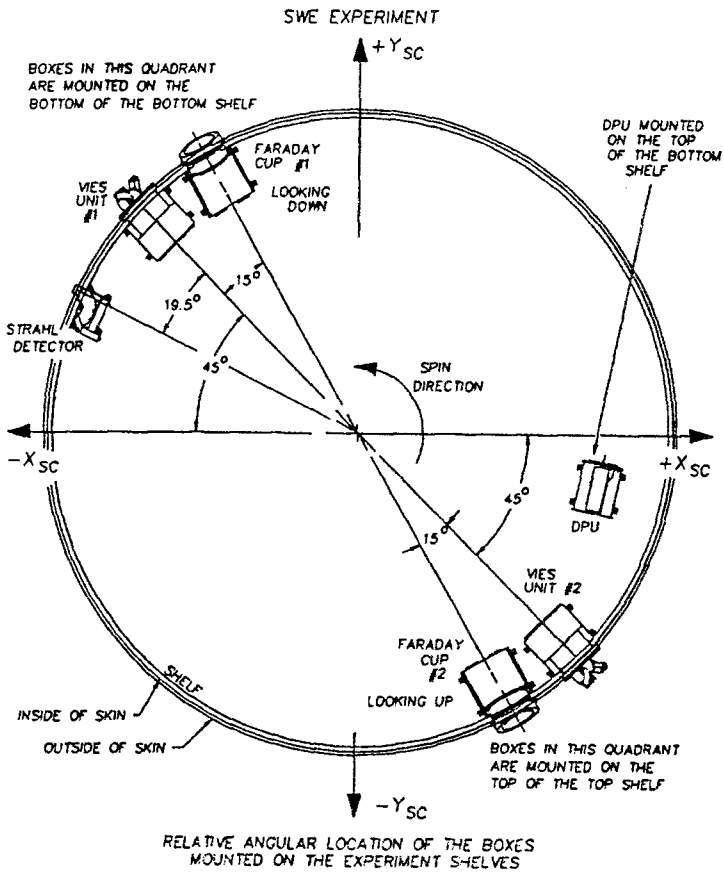
Fig. 2.   The arrangement of the components of the SWE instrument on the WIND spacecraft.

TABLE II

Instrument characteristics

Faraday cup	Energy/charge range	150 V–8.0 kV
	Operating frequency	≈ 200 Hz
	Effective area/cup	35 cm^2
	$\Delta E/E$ narrow windows	0.065
	$\Delta E/E$ double windows	0.130
	Maximum window width	1 kV
	Equivalent geometrical factor	1.1×10^2 cm^2 sterad
Vector spectrometer	Energy/charge range	7 V–24.8 kV
(ions and electrons)	Analyzer FOV	$7.5° \times 6.5°$
	$\Delta E/E$	0.06
	Geometrical factor (per analyzer)	4.6×10^{-4} cm^2 sterad
	Minimum step dwell time	5 ms
	Analyzer constant	7:1
	Plate radii: inside	4.717 cm
	Plate radii: outside	5.443 cm
Strahl spectrometer	Energy/charge range	5 V–5 kV
	Analyzer FOV	$\approx 3° \times \pm 30°$
	$\Delta E/E$	0.03
	Minimum step time	30 ms
	Geometrical factor (per anode)	7×10^{-4} cm^2 sterad
	Plate radii: inside	5.40 cm and 14.4 cm
	Plate radii: outside	6.60 cm and 15.6 cm

New modes of operation will be developed and uploaded to the instrument after launch. The DPU also formats data for the telemetry and can calculate key parameters. The interface boards transmit DPU signals to the subsystems and receive information from the subsystems as shown in the block diagram, Figure 3. The DPU uses Sandia 3300 central processing, timing, and control units. Software includes a default mode which, though rather general, will provide a considerable scientific return, and other stored modes which can be activated by the transmission of time-tagged pointers. This flexibility means that mode changing can be done without the transmission of messages to the spacecraft.

3.3. THE VEIS

The VEIS is an instrument designed for determining in detail the distribution functions of ions and electrons over the energy/charge range from 7 V to 24.8 kV. It consists of two sets of three small electrostatic analyzers which are identical and employ balanced deflection through 127° in a cylindrically-symmetric electric field. One triad is shown in Figure 4. Ions and electrons are measured sequentially,
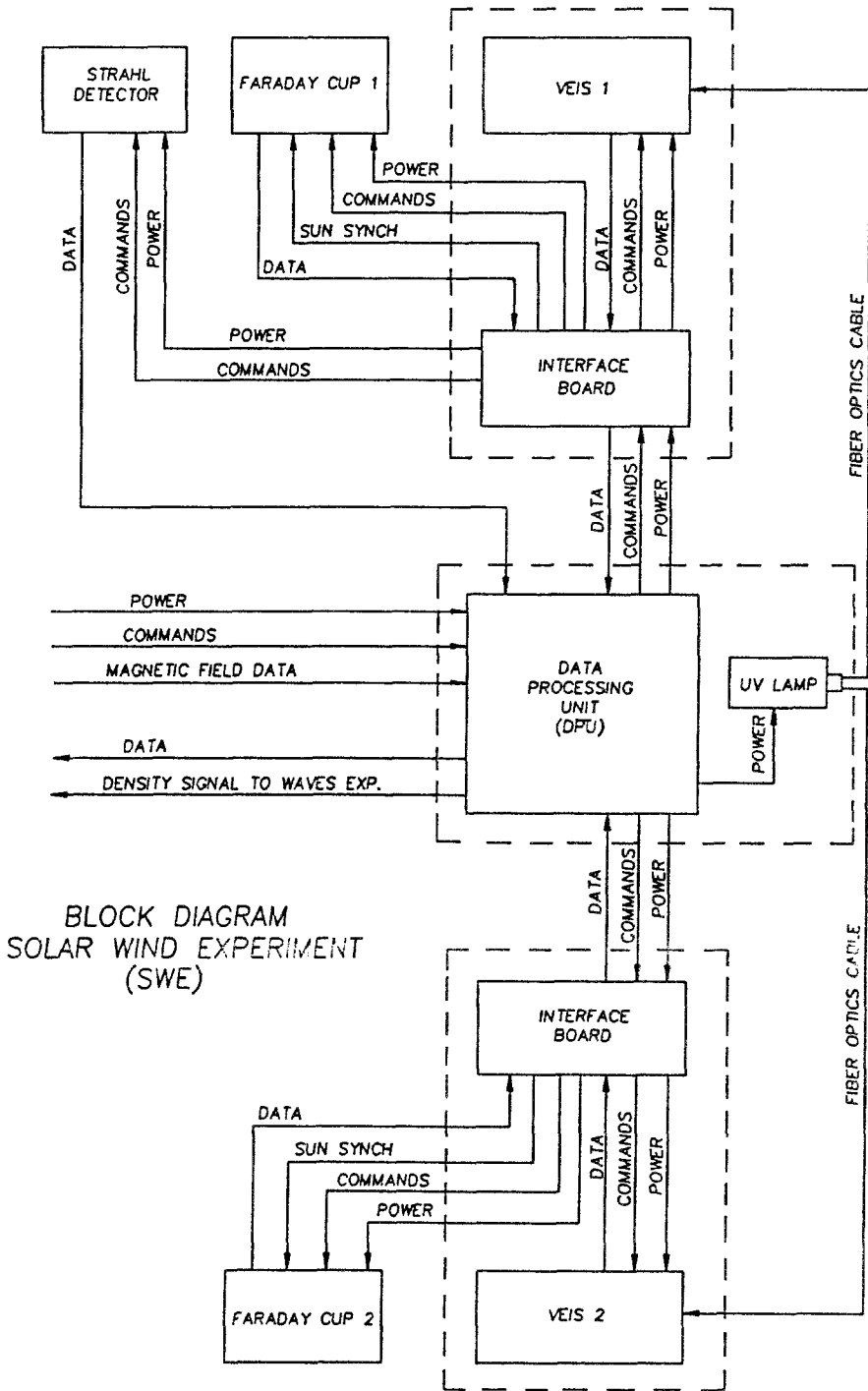
Fig. 3.   A block diagram of the instrument showing the signal flow. Note that the only interface between the spacecraft and the instrument for signals or power is through the DPU.

by reversing the direction of the analyzer electric field, and are detected by channel electron multipliers. In a similar way to the successful ISEE instrument, the field of view of each analyzer is determined solely by a collimator at the entrance and by the sensitive area of the detector. A mesh-covered hole in the outer plate is provided so that light can be trapped rather than scattered inside the analyzer. A high-transparency mesh grid placed between the exit slit and the channel multiplier detector prevents electric field leakage between the channeltron chamber and the analyzer. Other grids prevent low energy electrons formed on the channeltron cone from being drawn out. These design features result in an analyzer with very well defined transmission and solid angle properties, free from serious 'ghost' responses, and largely immune to responses resulting from photoelectrons produced inside the analyzer. As indicated in Figure 4 the calculated energy response of each analyzer is narrow, providing a differential energy window of $\Delta E/E \approx 0.06$ and a substantial geometric factor (4.6×10^{-4} cm^2 sterad). The energy-angle coupling of this proven design is much reduced as compared with a slitless analyzer system.

These analyzers have approximately $7.5° \times 6.5°$ fields of view; and using them to obtain 3-D coverage entails the assumption that each direction of view is representative of a larger angular region, i.e., each of the six analyzers must represent approximately $4\pi/6$ steradians. This condition is satisfied for plasmas having flows with Mach number $M \leq 1$. By using analyzers looking in opposite senses along mutually perpendicular axes, the flow direction and other moments can be obtained in an elegant way. Electrons in the solar wind which have flows with $M \leq 1$ can be accurately observed using such a triad, as was done on ISEE-1 and will be extended on the WIND spacecraft to include diffuse ions. Although flows with higher Mach numbers will not be missed using such a detector, to characterize them accurately requires the use of a larger number of narrow-angular-response analyzers, as will be done on the POLAR spacecraft with the HYDRA instrument and the strahl detector.

On a spinning spacecraft the spin causes the observations to be made along a curved path in velocity space. If six energy scans of 16 points are made every 60° of spacecraft rotation, each distribution function obtained by the six detectors contains $6 \times 16 \times 6 = 576$ points; an example is shown in Figure 5. With multiple analyzers each having rigidly-defined solid angles of acceptance, there is no possibility that an omni-directional background flux can be confused with the desired directional flux.

Two channeltron detectors are provided per analyzer, one each for electrons and ions; they are each equipped with a cone to match the output slit of the analyzer. The channeltrons are selected and qualified by established methods used previously. To avoid contamination and the resultant gain degradation, prelaunch nitrogen purging is employed. The mechanical construction of the instrument prevents gases emitted under vacuum from the electronics boards from passing through to the detector compartment. The detectors are mounted on ceramic circuit boards with AMPTEK A-111 charge-sensitive preamplifiers, having both digital and ana-
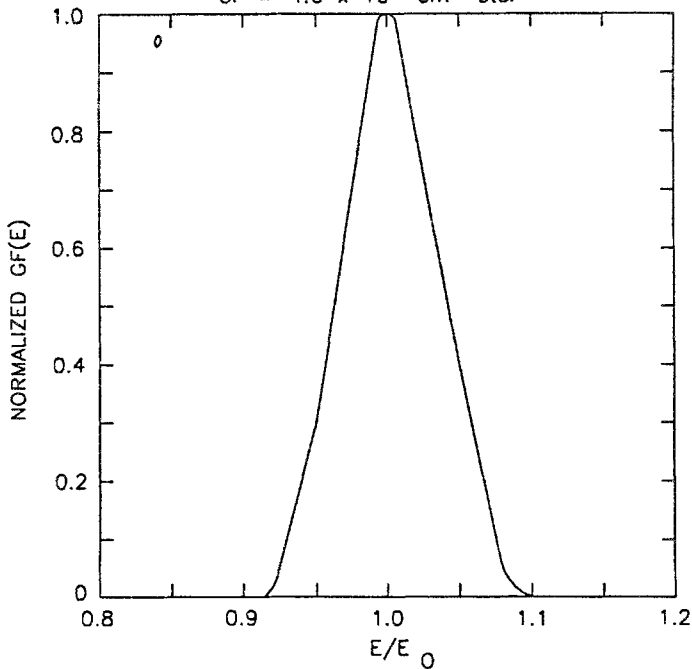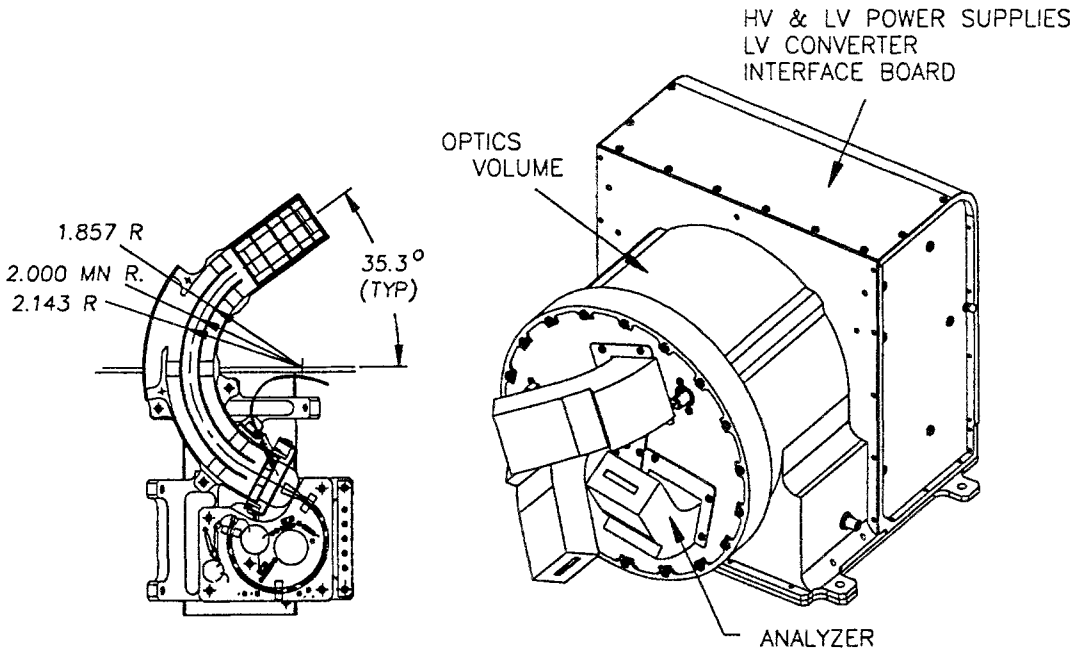
Fig. 4. A diagram of the vector electron and ion spectrometer showing the response of one analyzer. At top left we show a cross section of one analyzer and its associated electronics. The electronics are isolated from the detectors and are located in the 'optics' volume. There is another detector hidden by the one shown. In the lower portion of the figure, we show the response of one analyzer. The full geometrical factor (GF) is 4.6×10^{-4} cm^2 ster^{-1}.
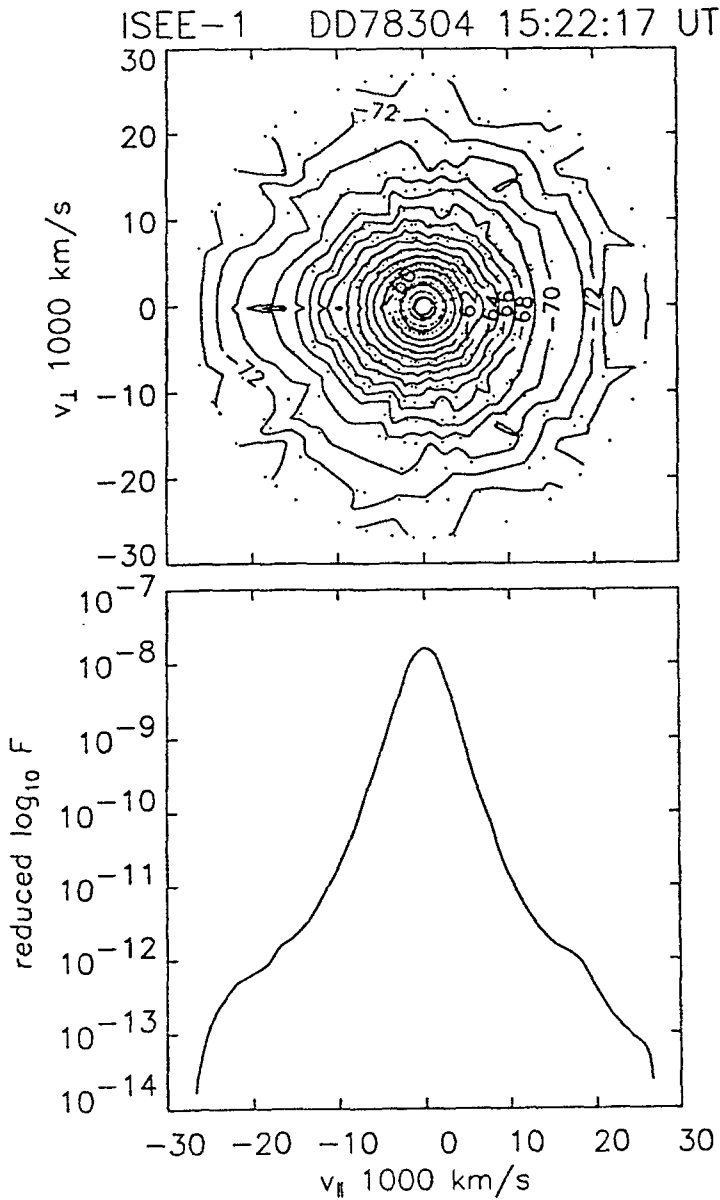
Fig. 5. A typical reduced distribution function derived from the electron spectrometer on ISEE 1. We expect to obtain similar functions from the SWE instrument, except that a gap, apparent in the upper diagram as a shortage of observations (points) along the magnetic field direction will be closed by the use of the strahl detector.

log pulse outputs. The latter will periodically be subjected to pulse height analysis, to ensure that the detectors remain gain-saturated. These precautions represent

more rigorous protection than was used for ISEE, which nonetheless lasted for twelve years and accumulated over 2×10^{11} counts.

Figure 4 shows details of the construction of the analyzers. The voltage supply which provides the deflection field is bi-polar and symmetric; the potential is reversed between electron and ion scans, using a shunt regulator circuit in which the leakage current of a high voltage diode is controlled by illuminating it with an LED (Loidl, 1984).

3.3.1. *The UV Calibrator*

To reduce data from the VEIS, it is important that the relative gains of the six detectors be known to an accuracy of approximately 1%. To achieve this goal, each detector can be excited by UV photons, which are carried from a single lamp to each of the six analyzers by optical fibers. The UV lamp is driven by a 2 W rf oscillator which will be turned on for a short period every month. This system provides a stable relative calibration for all detectors.

3.4. THE FARADAY CUP SUBSYSTEM

The Faraday cup subsystem is used to determine distribution functions and basic flow parameters of the ion component of the solar wind; the sensors operate in a different way and have different properties from the electrostatic analyzers of the VEIS. Each sensor consists of a cup containing a set of planar grids and two, semi-circular collector plates onto which a selected portion of the solar wind impinges; the corresponding electric current due to positive ions is measured. Figure 6(a) shows a cross sectional view of one sensor. In order to determine the energy of the incoming ions and also to discriminate between the charged particles and the photoelectric current produced by sunlight, a selected portion of the charged particle flux is chopped at 200 Hz by means of a time-varying positive potential applied to a highly-transparent metal grid. Figure 6(b) illustrates the principle of operation. The time-varying potential is generated by a modulator, which produces a dc-biased, 200-Hz square wave. The resulting waveform can then vary from V to $V + \Delta V$, where $V + \Delta V$ can be as high as 8 kV and ΔV as large as 1 kV. The resulting chopped current from each collector is synchronously detected and integrated on a capacitor for a fixed time interval. The resulting voltage is converted to a digital signal using a logarithmic A/D converter.

The Faraday cup sensor system has at least four advantageous properties.

(1) Since ΔV is variable, the energy/charge bandwidth of the detector is variable, whereas it is fixed by geometry in the case of an electrostatic analyzer. This flexibility will be useful for the study of reflected ions, and for automated modes in which the peak of the solar wind distribution can easily be located.

(2) The flow direction can be determined to better than one degree. Knowledge of the flow angle to a high accuracy is necessary when interpreting measurements
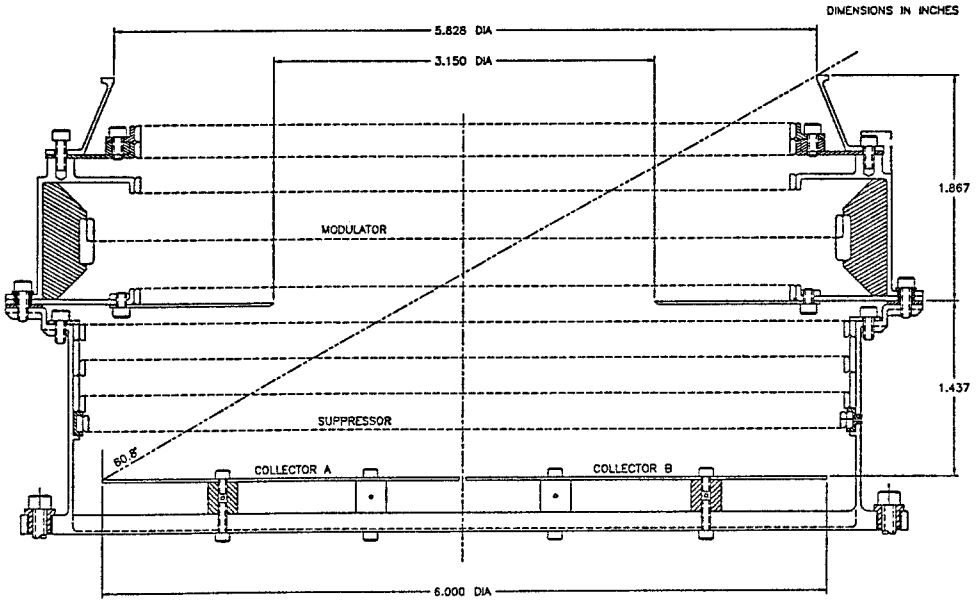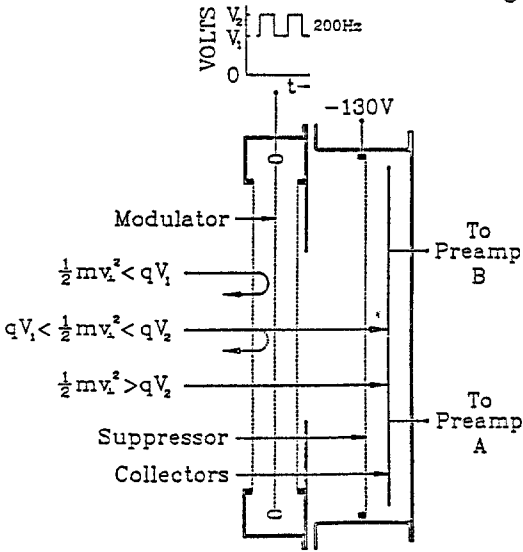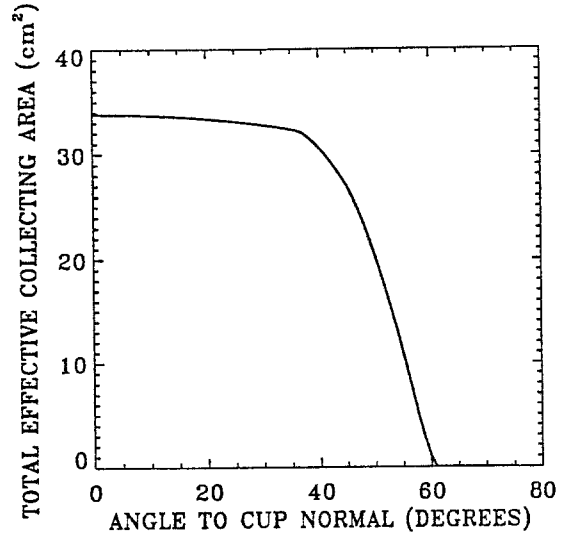
Figure 6a

Figure 6b

Figure 6c

Fig. 6. (a) A cross section of a Faraday cup sensor. All grids are at spacecraft ground potential except for the modulator grid (which has a time-varying voltage applied to it) and the suppressor grid which is biased at −120 V to prevent escape of secondary electrons from the collector plates. The grounded grids between the modulator grid and the collector plates are used to reduce capacitively-coupled currents due to the time-varying modulator voltage. The two outermost grids are used to reduce emission of time-varying electric fields from the front of the sensor. The maximum entrance angle of a particle is shown, neglecting refraction effects due to voltages on the grids. (b) A schematic cross section of a Faraday cup, showing the principle of operation (see text). (c) The effective area of the Faraday cup as a function of the incoming angle of a cold (parallel) beam of ions. The area is determined by internal apertures and the image of the beam on the full collector plate (the sum of both collector halves is used). The transparencies of the meshes have been taken into account.

made by other spacecraft in the magnetosphere and the magnetosheath as well as for determination of the properties of the bowshock and interplanetary shocks.

(3) The Faraday cup is well suited to measurements at high time resolution, even when used on a spinning spacecraft. It has a large sensitive acceptance angle (approximated by a 60° half-angle cone, see Figure 6(c)). Since we are using two cups facing in opposite directions at the ends of a spacecraft diameter, the solar wind is being measured 2/3 of the time, and variations in the full velocity distribution function can be observed with a time resolution of approximately one second.

(4) The Faraday cup provides measurements of the velocity distribution function integrated over directions perpendicular to the sensor's axis, i.e., measurements of the 'reduced' distribution function. From measurements of the reduced distribution function along several different look directions, the 3-D velocity distribution can be characterized. Such measurements can be transmitted to the ground with less telemetry than would be required by a pixel-type instrument. The Faraday cup is also particularly suitable for absolute density determinations in the supersonic solar wind since it can encompass the whole distribution and has no energy-dependent efficiency corrections.

3.4.1. *The Faraday Cup Current Signals*

As discussed above, a modulated voltage selects particles whose component of velocity perpendicular to the modulator grid lies in a selected range. Thus, a mono-energetic beam with energy/charge equal to the central energy/charge of the modulating window would be detected if it were normally incident on the sensor. But if it entered the sensor at a sufficiently large angle to the normal due, for example, to rotation of the sensor on a spinning spacecraft, it would not be able to pass through the grid. To demonstrate this dependence on angle as well as energy/charge, we show in Figure 7 the amplitude of the chopped (or 'modulated') currents resulting from a modeled solar wind distribution that has a bulk speed of 400 km s^{-1} and a velocity width of 40 km s^{-1}. The panels show the currents vs. azimuth angle of the spacecraft for a sequence of modulator windows ranging from below to above the speed of the wind.

The velocity range of each window for normally-incident protons is indicated in the upper right corner of each panel. The mean velocities increase from the top to the bottom panels of the figure. Consider first the currents measured at 0°, where the sensor is facing into the incoming flow of plasma. From the top to the bottom panel, the current at 0° increases and then decreases as the window velocity range passes over the velocity distribution of the wind.

Next, consider the currents measured when the sensor axis makes an angle to the incoming wind. The component of wind velocity normal to the modulator grid will be smaller, and thus the wind can be modulated by a window of lower voltage. The top panel illustrates such a case. The parameters that characterize the particle velocity distribution can easily be extracted from such a set of data. The spin-plane
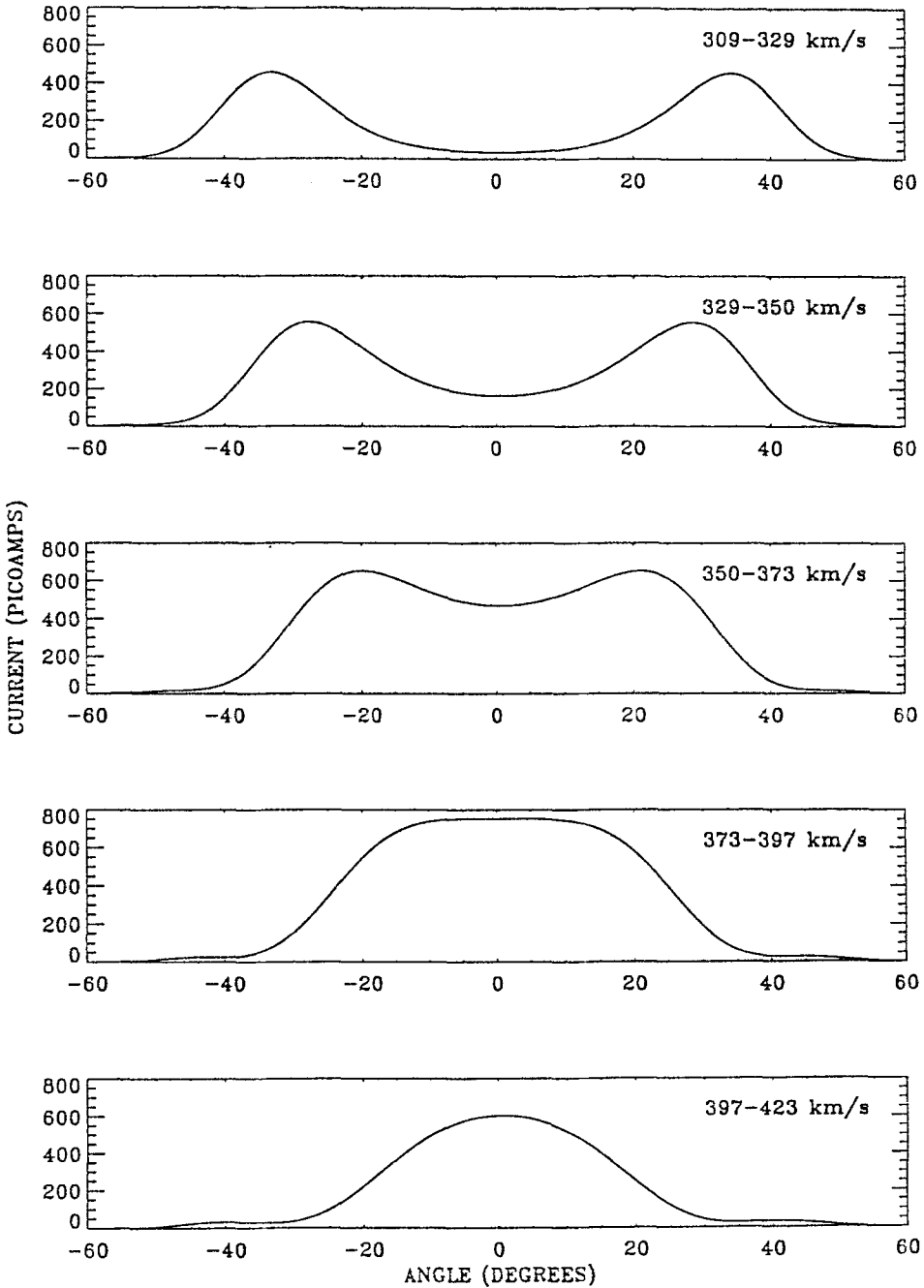
Fig. 7. Simulated Faraday cup currents vs azimuth angle for a 400 km s^{-1} bulk speed and 40 km s^{-1} most probable thermal speed solar wind containing 10 protons cc^{-1} and 0.5 α particles cc^{-1}. For any particular angle, a plot of current versus energy will have two maxima, one for the protons and one for the alpha particles. The energy windows in which the current maxima occur are a function of the angle of the incoming plasma flow to the sensor normal direction. The currents due to alpha particles peak in an energy window higher than shown here, but they are just visible at large angles in the bottom panel.

angle from which the flow comes is determined from the azimuth angle at which the peak current is measured. The speed, density, and temperature of the wind can easily be determined by taking weighted moments of the currents measured in each energy window. Using a model velocity distribution, a nonlinear, least-squares fit to the currents can be performed to extract the maximum amount of information from the measurements.

The elevation angle of the flow can be determined from the relative currents measured by the two sensors, since one sensor normal is tilted 15° above the spin plane of the spacecraft and the other normal is 15° below that plane. An alternative technique is to make use of the relative currents from the two halves of the collector plate in a single cup.

The double-peaked current produced using only one window just below the peak of the velo- city distribution can be used to obtain information about the distribution in a single spacecraft rotation ($\approx$ 3 s for WIND). The angular separation of the peaks determines how far the window is below the bulk velocity of the distribution, and the width of the peaks is a measure of temperature of the distribution. Our simulations show that this technique can provide accurate distribution parameters, and we plan to explore the use of this 'single-spin', mode on WIND to obtain parameters with high time resolution.

3.4.2. *The Faraday Cup Measurement System*

Figure 8 shows a block diagram of the Faraday cup measurement system. The modulator can supply the required dc-biased, square-wave voltage waveform between any two of 64 logarithmically-spaced voltage levels ranging from 150 to 8000 V. The velocity resolution of a single window is $\Delta v/v \approx 0.033$. Normally, we intend to use 'double-width' windows with a voltage waveform going from level n to level (n+2), thus generating velocity windows with $\Delta v/v \approx 0.065$. The voltage window will be maintained for a full revolution of the spacecraft; and in the 'full-scan' mode, 31 velocity windows can be scanned in 93 seconds at a nominal spacecraft spin rate of 3 s/revolution^{-1}. In a more-efficient 'tracking' mode, 14 windows will be chosen to cover a velocity range that includes the window that had the peak current in the previous scan; the time for a scan in this mode will be approximately 42 s. A full-scan will be taken every 30 min, to insure that we are not tracking a spurious peak. A full-scan will also be initiated if the maximum observed current is less than a pre-determined threshold.

The modulated currents from each half collector plate are measured by independent measurement systems. The currents are capacitively coupled to a preamplifier (bandwidth $\approx$ 200 Hz, centered at 200 Hz). The preamp's output is fed to three range amplifiers connected in series. (Their gains from the first to the third are 7, 46.5, and 46.5.) The output of each range amplifier is synchronously detected and the resulting dc signal is integrated on a capacitor for an integral number of periods of the 200 Hz modulating waveform, nominally for 30 ms. At the end of the integration period, a multiplexor sequentially searches for the highest- gain,
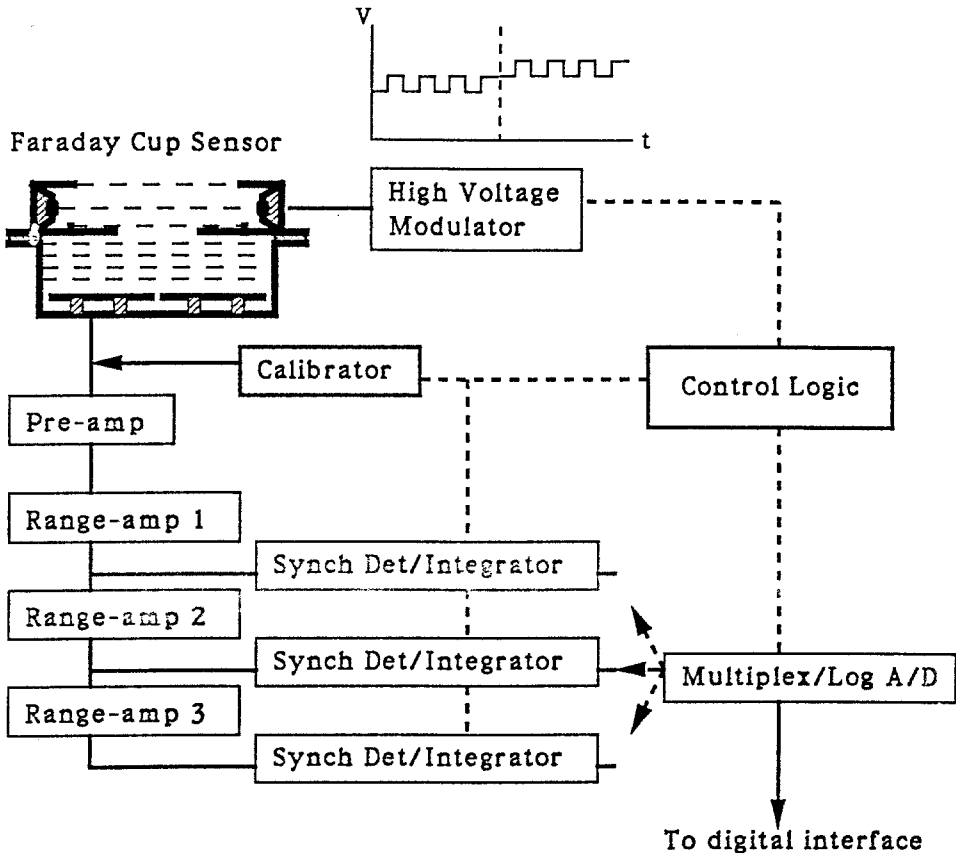
WIND SWE Faraday Cup Subsystem

Fig. 8. A block diagram of the Faraday cup portion of the SWE instrument.

unsaturated output. That output is then logarithmically converted to a 10-bit digital number. When combined with two additional bits specifying the range amplifier used, the net dynamic range of the system is 105. A 30 ms integration time will allow measurement of currents in the range from 3×10^{-13} to 3×10^{-8} amps. The thermal noise level for that integration time is 3×10^{-13} amps. In our nominal mode of operation, the integration time is increased to 120 ms for angles when the cup is looking away from the Sun.

The combined data rate from both FC sensors is 320 bits s^{-1}. The total times required to obtain a spectrum in each sensor using the 'full-scan' and 'tracking' modes are 93 and 42 s, respectively. As mentioned earlier, we intend to explore the use of a 'single-spin' mode which should give us information about the velocity distribution function in either a full- or half-spin period depending upon whether both cups are used to determine the longitudinal flow angle or whether information

from a single cup with its split collector is sufficient. The fully re-programmable DPU allows us to adjust our data-taking modes to suit the charac- teristics of the region being observed.

3.5. THE 'STRAHL' DETECTOR

A magnetic-field-aligned beam or strahl in the solar wind electron velocity distri-bution results partly from the velocity dependence of the cross section for electron coulomb collisions. As a result of the rapid fall-off in density and hence the number of collisions as one moves outward in the corona, electrons with energies above approximately 40 eV moving along the magnetic field can travel to 1 AU with little scattering. Thus observations close to the field direction sometimes detect the presence of a 'strahl' of higher energy electrons. The properties of this feature of the solar wind electron distribution have been studied between 0.3 and 1 AU from the Helios spacecraft (Marsch *et al.*, 1991), but further observations at 1 AU over an extended period of time will increase our knowledge of the forrnation and prop-erties of this structure. To do so requires an angular resolution of a few degrees, and that measurements be performed in an angular region of size $\approx 30° \times 30°$ centered on the magnetic field direction. The WIND strahl detector is a truncated, toroidal electrostatic analyzer with an included angle of $131°$ (Young *et al.*, 1987), see Figure 9. This device covers a field about $\pm 28°$ in a plane containing the spin axis. The detectors are two channel plates. As shown in Figure 9, six anodes, covering approximately $5°$ each, are used per plate. They are read out commencing $16°$ after the solar direction every 31 ms until $72°$ after the solar direction. This sequence of 15 observations is repeated when the spacecraft has made a half revolution and is looking along the magnetic field in the anti-Sun direction. Although the magnetic field direction shows considerable fluctuations, it will be within the field of view of this sensor approximately 60% of the total observing time. Note that there is no detector on which sunlight can directly fall, since the center anode and channel plate are absent. The outer plate of the analyzer is serrated to minimize reflected light. In general, the proper operation of this part of the instrument depends upon the alignment of the spin axis of the spacecraft at right angles to the ecliptic plane. The channel plate technology, which is well understood, requires rigid attention to cleanliness and to the purging of the instrument with dry gas before launch. Both channeltrons and channel plates were installed after the spacecraft thermal vacuum test to avoid contamination.

4. Modes of Operation

In this section we gather together descriptions of the modes of operation that exist before launch and some modes that are in the planning stage at the time of this writing. Note that additional modes will be telemetered to the DPU after launch. The modes are described below.

PRE-AMP
BOARDS

MCP POWER
SUPPLY

TOROIDAL
ANALYZER

MCP
AREA

STEPPING
POWER
SUPPLY

ANODES

MCP

TOROIDAL
PLATES

BASE
PLATE

APERTURE

APERTURES

AZ.

EL.

CHEVRON
MCP STACK

30

RESPONSE

DEGREES

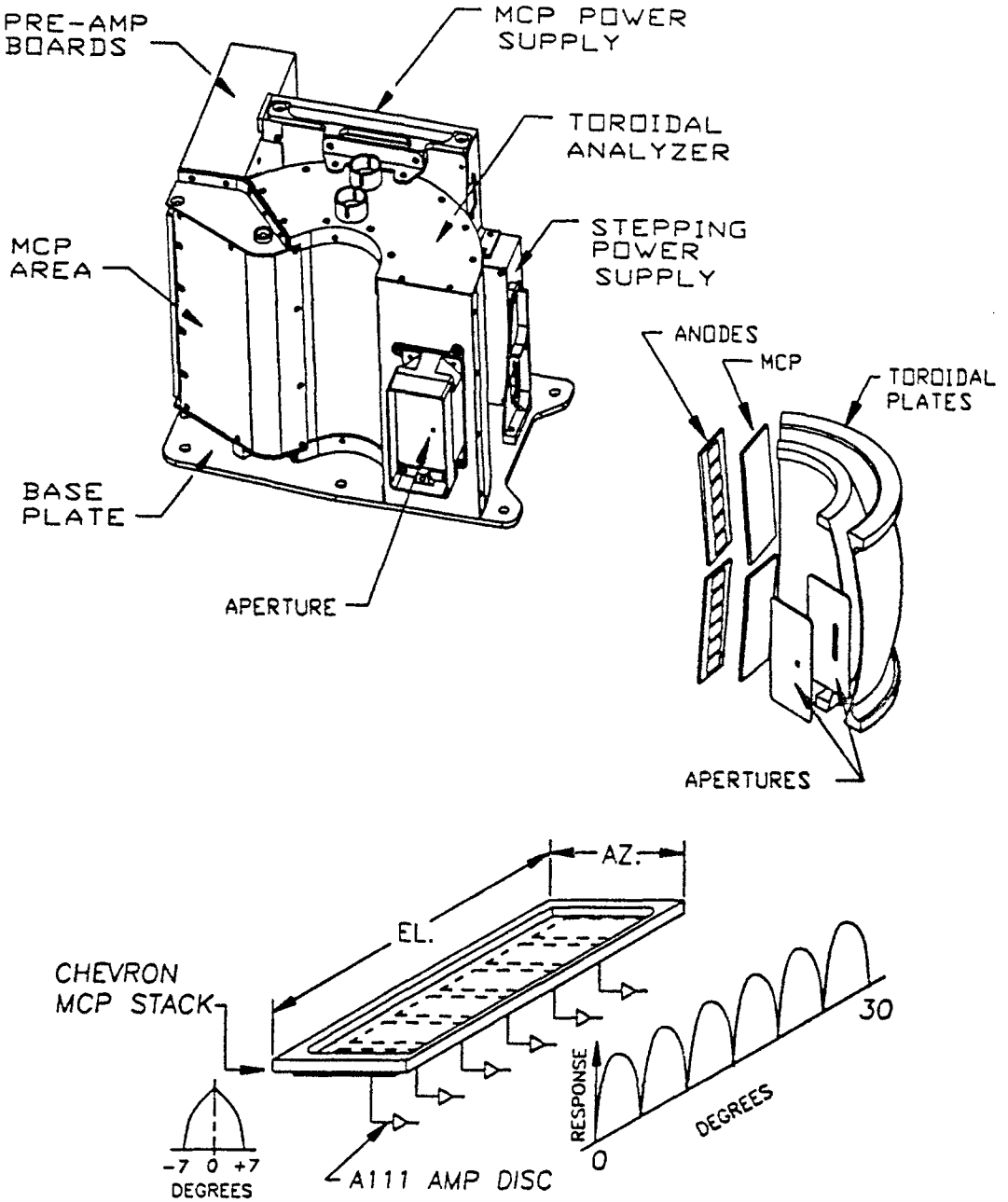-7 0 +7
DEGREES

A111 AMP DISC

0

Fig. 9.   A diagram of the strahl sensor. The analyzer uses toroidal plates, which focus particles approaching the slit onto two microchannel plates with six anodes each, as shown in the lower part of the diagram. Each anode has its own preamplifier.

4.1. MODE 0

This mode is permanently stored in the ROMs of the DPU. It is intended as a survival mode that is used initially and then superseded by more specialized modes. Its purpose is to provide a basic scan of the energy and angle ranges available to the SWE sensors and also to transmit those observations in a limited number of major frames of the spacecraft telemetry.

In this mode, the FC makes observations using one 'double' energy window each spin. The windows energies are sequentially increased, and 28 spins are used to scan a reduced energy/charge range: from 150 to 5478 V. An additional spin is used to calibrate the measurement chains using one of 12 input currents. During each of the spins, measurements are made using specific integration times that are multiples of the modulation period (approximately 5 ms). When a cup looks within $\approx \pm 60°$ of the spacecraft-Sun line, ≈ 30 ms times are used; and ≈ 120 ms integration times are used when the particular cup faces outside that angular range. Each spin, the data-taking sequence is triggered at a fixed angle relative to the Sun, and for the nominal spin rate, the set of narrow sectors is centered 4° before the Sun-direction to take account of the nominal wind aberration angle. To reduce the data rate, every other narrow sector is used and only two wide-angle sectors are used per sensor. The equivalent angles over which the currents are averaged are 3.61° and 14.45° at the nominal 3 s spacecraft spin rate. (Fixed integration times are used to minimize noise effects.)

The VEIS and strahl subsystems make measurements over fixed angular intervals using the spacecraft-provided sectored spin pulses. During each 60° sector of a spin, 16 sequentially-increasing VEIS energy steps are used; counts for each energy window are accumulated over approximately 3.53° ($\frac{1}{17}$ of the sector); the sequence of levels is reinitiated at the start of the next 60° sector. Fourteen 60°/17 samples at one energy level are taken by the strahl sensor centered on the nominal 45° spiral angle of the magnetic field; the samples are taken twice per rotation: in both directions along the field line. The strahl energy steps are sequentially increased each spin; 16 spins are required to cover the entire energy range.

4.2. MODE 1

A general purpose mode, Mode 1, is an extension of mode 0, but it resides in the EEPROMs and can be altered easily by ground command. As currently implemented, the Faraday Cup system will cover the full energy/charge range, and a full set of calibration currents can be injected in contiguous spins. In the foreshock the VEIS energies can be selected to alternately measure electrons and ions with a time resolution of six seconds. Thus Mode 1 allows for example, characterization of foreshock and solar wind ions and electrons and the strahl as well as the diffuse ions and electrons from the bow shock in less than one minute. This time resolution

will be important for our studies of the region between the bow shock and $L1$, described in Section 2.3.

4.3. OTHER MODES

Planned modes, not completely implemented at this writing, include the 'burst' mode described above, which can capture transient phenomena; a 'tracking' mode in which a limited number of FC energy/charge windows are chosen to track the center of the solar wind velocity distribution and thus yield parameters with higher time resolution; and a 'single-spin' mode in which the Faraday Cup energy/charge window is chosen to be just below the peak of the distribution function and measurements are taken in a single spin as described in Section 3.4.1.

Acknowledgements

References

Belcher, J. W., Lazarus, A. J., McNutt, R. L., Jr., and Gordon, G. S.: 1993, 'Solar Wind Conditions in the Outer Heliosphere and the Distance to the Termination Shock', *J. Geophys. Res.*, to be published.

Bellomo, A. and Mavretic, A.: 1978, *MIT Plasma Experiment on IMP H and J Earth Orbited Satellites*, MIT Center for Space Research Technical Report CSR-TR-78-2, 1978.

Bridge, H. S., Belcher, J. W., Butler, R. J., Lazarus, A. J., Marvetic, A. M., Sullivan, J. D., Siscoe, G. L., and Vasyliunas, V. M.: 1977, 'The Plasma Experiment on the 1977 Voyager Mission', *Space Sci. Rev.* **21**, 259.

Loidl, A.: 1984, 'HV Diodes Used as Variable Resistors and Switches', *J. Phys. E: Sci. Instruments* **17**, 357.

Marsch, E.: 1991, in R. Schwenn and E. Marsch (eds.), *Physics of the Inner Heliosphere*, Vol. II, Springer-Verlag, Heidelberg, p. 45.

Ogilvie, K. W., Scudder, J. D., and Doong, H.: 1978, 'The Electron Spectrometer on ISEE-1', *ISEE Transactions on Geoscience Electronics GE-16* **261**.

Scudder, J. D. and Olbert, S.: 1979a, 'A Theory of Local and Global Processes which Affect Solar Wind Electrons. 1. The Origin of Typical 1 AU Velocity Distribution Functions–Steady State Theory', *J. Geophys. Res.* **84**, 2755.

Scudder, J. D. and Olbert, S.: 1979b, 'A Theory of Local and Global Processes which Affect Solar Wind Electrons. 2. Experimental Support', *J. Geophys. Res.* **84**, 6603.

Vasyliunas, V. M.: 1971, 'Deep Space Plasma Measurements, 12.1', *Methods of Experimental Physics* **98**, 49, Academic Press, New York.

Young, D. T., Ghielmetti, A. G., Shelley, E. G., Marshall, J. A., Burch, J. L., and Booker, T. L.: 1987, 'Experimental Tests of a Toroidal Electrostatic Analyzer', *Rev. Sci. Instrum.* **58**, 501.